

# RELAXATION-INDUCED PIEZORESISTIVITY IN CARBON-BASED MONOFILAMENT HIERARCHICAL POLYMER COMPOSITES

A. Can-Ortiz<sup>1</sup>, F. Avilés<sup>1</sup> and J. L. Abot<sup>2</sup>

<sup>1</sup> Centro de Investigación Científica de Yucatán A.C., Unidad de Materiales, Calle 43 No.130 x32 y 34, Col. Chuburná de Hidalgo. C.P. 97205, Mérida, Yucatán, Mexico.

<sup>2</sup> Department of Mechanical Engineering, The Catholic University of America, Washington, DC 20064, USA.

**Keywords:** Viscoelastic phenomena, structural health monitoring, hierarchical composites.

## ABSTRACT

The use of multiscale carbon nanostructures to self-sense viscoelastic phenomena in monofilament polymer composites using the electrical resistance method is explored, investigating the behavior of glass fibers modified with multiwall carbon nanotubes (GF-CNT), carbon nanotube fibers (CNTF) and conventional carbon fibers (CF) embedded in a thermosetting vinyl ester matrix (VER). The results of the relaxation-induced piezoresistivity tests of monofilament composites showed that the electrical resistance of the CF/VER system increases with elapsed time, whereas that of CNTF/VER and GF-CNT/VER decreases with time, in response to the stress relaxation behaviour. Changes in the electrical resistance demonstrate that these multiscale materials can be used for self-sensing of viscoelastic phenomena by monitoring their electrical resistance, and that its electric response upon polymeric relaxation is strongly dependent on the fiber architecture and its nanostructure.

## 1 INTRODUCTION

The interest in hierarchical multiscale composite materials have recently increased in multifunctional and specialized applications within the aerospace industry [1], construction [2] and marine applications [3], among others; because of this, knowledge of their structural health in real time and of the reversible and irreversible mechanical and molecular phenomena occurring within the material can be a critical factor for their damage assessment, and for boosting their potential applications. Although the study of deformation and damage incurred by quasi-static loading may be the starting point for these multiscale hierarchical materials, in many applications these polymer composites are subjected to constant stress or strain for prolonged time periods, rendering high relevance to viscoelastic phenomena. In this way, a complete monitoring of the structural health of an advanced composite material to prevent catastrophic failures requires sensing of mechanical phenomena incurred not only for quasi-static and dynamic loading, but also by viscoelastic issues. In the case of polymer composite materials formed by electrically conductive fibers such as conventional carbon fibers [4,5] or CNT fibers or “yarns” [6], self-monitoring of quasi-static loading has been carried out through the piezoresistive effect induced by such fibers embedded into the composite, i.e. by the change in the effective electrical resistance of the composite due to an applied stress/strain [4-6]. However, when the fiber is not electro-conductive (as for the case of glass and aramid fibers) application of this principle for composites with non-conductive polymer matrices is not possible without using an additional electro-conductive filler. For this case, polymer matrices reinforced with electrically insulating fibers have been modified with electrically conductive nanostructures such as carbon nanotubes, rendering piezoresistivity [1,3,7,8]. It has been shown that when insulating fibers are modified with CNTs and subsequently embedded in a polymer matrix, they can be used as non-invasive sensors for deformation and damage of their composites in real time [9-11]. Given this background, this work reports the ability to self-sense viscoelastic phenomena through changes in the effective electrical resistance of monofilament composites comprising three kinds of fibers, glass fibers modified with CNTs, CNT yarns and, as reference material, conventional carbon fibers.

## 2 MATERIALS AND METHODS

### 2.1 Materials

For glass fibers modified with carbon nanotubes (GF-CNT), commercial multiwall carbon nanotubes (MWCNTs) from CheapTubes Inc. (Vermont, USA) with 30-50 nm outer diameter, 5-10 nm inner diameter, purity >95%, and 1-6  $\mu\text{m}$  length [12] were used to modify the glass fibers. The MWCNTs were oxidized using a solution of  $\text{H}_2\text{SO}_4/\text{HNO}_3$  at 3.0 M (3.0 M each acid) for 2 h, following the procedure reported in [13]. The glass fibers (GF) used were commercial E-glass fibers with an average diameter of 15  $\mu\text{m}$ , density of 2.54  $\text{g}/\text{cm}^3$ , extracted from fiber tows containing ~4000 filaments per tow [14]. The MWCNTs were deposited on the GF by using an electrophoretic deposition method with an electric field of 4.5 kV/m with a deposition time of 30 min at 50 °C. Carbon nanotube fibers/yarns (CNTF) used in this study were synthesized at the “Nanoworld Laboratories” of the University of Cincinnati (Cincinnati, USA); The CNTF were dry-spun from the sides of 500  $\mu\text{m}$  high vertically aligned arrays composed of 15 nm diameter MWCNTs grown by water-assisted chemical vapor deposition. The yarns have an average diameter of ~46  $\mu\text{m}$ , a density of 0.65  $\text{g}/\text{cm}^3$  and the twist angle is about 30° [6,15]; using the relationship between twist angle and porosity reported in [16], their estimated porosity is around 0.63. Commercial carbon fibers (CF) TR30s were acquired from “Mitsubishi Rayon Carbon Fiber and Composites Inc.” (CA, USA) with an average diameter of 7  $\mu\text{m}$  and density of 1.79  $\text{g}/\text{cm}^3$ , extracted from fiber tows containing ~3000 filaments per tow. For composite manufacturing, a vinyl ester Hetron 992 FR resin (VER) from Ashland composites (Ohio, USA) was used as the polymer matrix. Cobalt naphthenate in a proportion of 0.2 wt % and 0.6 wt % of methyl ethyl ketone peroxide were mixed with VER to manufacture the composites.

### 2.2 Morphological characterization of the fibers

Scanning electron microscopy (SEM) was conducted to investigate the morphology of the three fibers (GF-CNT, CNTF and CF), using an accelerating voltage of 20 kV in a JEOL JSM- 6360LV equipment. For GF-CNT and CF, the samples were extracted from fiber tows and for CNTF individual fibers were provided and chosen for SEM imaging. The samples were fixed on an aluminum support and gold-sputtered before SEM analysis.

### 2.3 Manufacturing process of monofilament composite materials

The composite materials examined in this work consisted in three groups of monofilament composites, containing a single fiber (GF-CNT, CNTF or CF), as shown in Fig. 1. The monofilament composites were denominated GF-CNT/VER, CNTF/VER or CF/VER, depending on the fiber used.

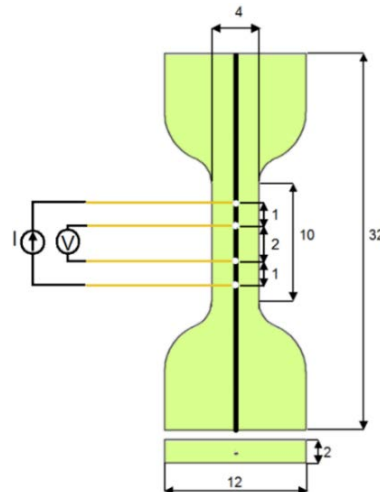


Figure 1: Schematic of monofilament composites used for the electromechanical characterization upon stress relaxation. Dimensions in mm.

The monofilament composites were prepared by the following procedure. First, four electrodes were fixed to the silicone mold through tiny holes specially made for this purpose; these electrodes were defined in order to conduct four-point electrical measurements, and consisted of a 40 gauge copper wire centered in the plane of the specimen and defined at its mid-thickness. The pair of current injection electrodes (external electrodes) were centered 4 mm apart, while the pair of voltage electrodes (internal electrodes) were centered 2 mm apart. Subsequently, an individual fiber was lied over the copper wires in the same plane defined by the four electrodes but perpendicular to them (see Fig. 1) and affixed to the copper wires by using conductive carbon paint (water-based dispersion of carbon particles in natural resin) from “Bare Conductive Limited” (London, United Kingdom) to ensure electrical contact. For the resin preparation, 5 g of VER was mixed with 10 mg of cobalt naphthenate using mechanical stirring for 3 min, and subsequently with 30 mg of ethyl methyl ketone peroxide mixing for another 3 min; then vacuum was applied for 1 min, and the VER was poured into the mold containing the individual fiber, allowing for 24 h curing. Finally, the specimens were demolded and post-cured in a convection oven at 60° C for 1 h, increasing the temperature to 80° C during the second hour, and finally to 100° C for 2 h more. A total of three specimens were fabricated for each material system.

#### 2.4 Piezoresistive characterization on relaxation test of monofilament composites

A Shimadzu AGS-X universal testing machine was used for mechanical stress relaxation tests, using a 1 kN load cell as a force sensor. The stress( $\sigma$ )/strain( $\varepsilon$ ) program for the relaxation test is depicted in Fig. 2. Monotonically increasing strain was initially applied at a crosshead displacement rate of 0.8 mm/min until a time  $t_1$ , which corresponded to  $\varepsilon_0 = 0.4\%$  (measured with a stain gage centered at the back of the specimen). The strain  $\varepsilon_0 = 0.4\%$  was kept constant thereafter for 2 h ( $t_2$ ).

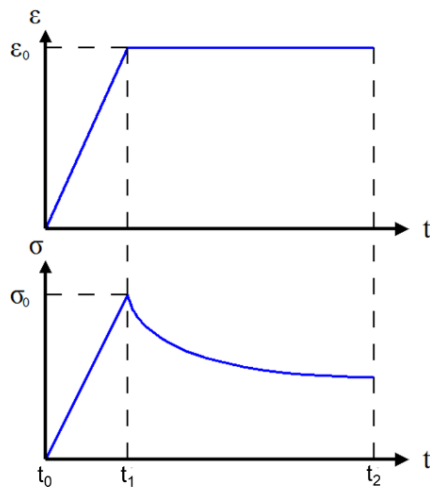


Figure 2: Steps of relaxation test applied to monofilament composites.

According to Fig. 2, the relaxation tests were performed using a constant strain level ( $\varepsilon_0$ ) of 0.4%, which corresponds to an initial stress ( $\sigma_0$ ) of 15 MPa. The loading process (at 0.8 mm/min crosshead displacement rate) initiated at time  $t_0$  until a stress ( $\sigma_0$ ) of 15 MPa (~ 40% of the ultimate stress) was reached. When the stress level reached  $\sigma_0$ , (at time  $t_1$ ) the crosshead displacement was stopped, keeping  $\varepsilon_0 = 0.4\%$  constant and monitoring the changes in  $\sigma$  through force measurements conducted by the load cell of the universal testing machine; the relaxation test was stopped at time  $t_2 = 2$  h. The electrical resistance of the specimens ( $R$ ) was simultaneously measured using the four-point technique by an Agilent B2911A precision source/measure unit with a constant current of 10  $\mu$ A, synchronizing all instruments using an in-house data acquisition software. For the data analysis,  $R_0$  corresponds to the initial electrical resistance of the monofilament specimen at  $t=0$ , and during the relaxation process (between  $t_1$  and  $t_2$ ) the fractional changes in electrical resistance were referenced to the value of the

electrical resistance corresponding to  $\varepsilon_0$  ( $t = t_1$ , just at the beginning of the relaxation process), which was named  $R_0^r$ . Thus, during the relaxation experiment, the fractional changes in electrical resistance,  $\Delta R/R_0^r = (R - R_0^r)/R_0^r$ , and the corresponding fractional changes in stress with respect to the value of the initial relaxation stress ( $\Delta\sigma/\sigma_0$ ) were recorded and plotted as functions of elapsed time ( $t$ ) for each test. Three monofilament specimens were tested for each material system.

### 3 RESULTS AND DISCUSSION

#### 3.1 Morphological characterization of the fibers

In order to obtain a morphological description of the materials used, SEM micrographs of CF (Fig. 3a), CNTF (Fig. 3b) and GF-CNT (Fig. 3c) are presented in Fig. 3.

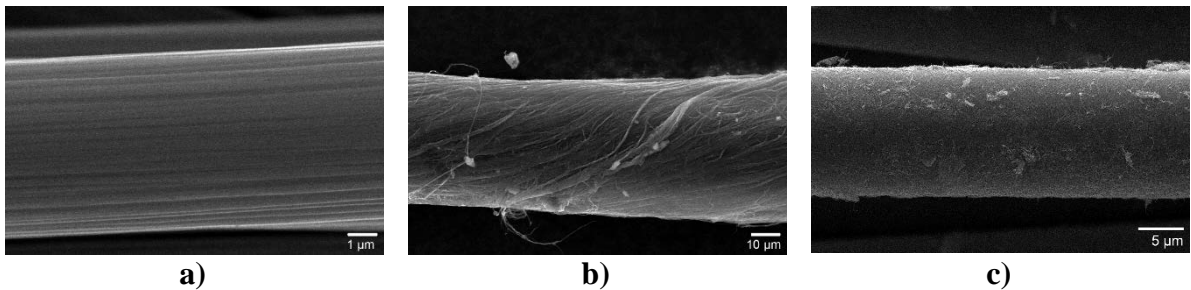


Figure 3: SEM micrographs of fibers used. a) CF, b) CNTF, c) GF-CNT.

In Fig. 3a it is observed that CF presents certain texture on its surface with grooves arising from the synthesis of PAN-based carbon fibers. This structure is due to the way in which the different layers of carbon that conform the fiber are oriented which depends on the conditions of fiber synthesis [17], such as temperature and spinning conditions [17]. On the other hand, Fig. 3b shows that the morphology of the CNTF is very different from that of CF; CNTF comprises millions of individual CNTs of limited length, twisted together (with a torsion angle of  $\sim 30^\circ$  in this case) to conform the fiber yarns. It can also be observed that the fiber is not a solid with a true continuous cross-section, but it contains empty spaces between the twisted CNTs that conform the fiber, which defines its porosity [16]. All these characteristics of the CNTF depend on their synthesis and processing conditions. Finally, the surface of the GF-CNT (Fig. 3c) presents a rather homogenous distribution of MWCNTs on the glass fibers surface, with a surface roughness dictated by the amount of MWCNTs deposited [18]. It has also been pointed out that bonding between such the (oxidized) MWCNTs and fiber surface is possible due to the presence of COOH and OH groups on the MWCNT surface, which interact with the C=O functional groups in the fiber sizing through the formation of hydrogen bonding, and/or esterification processes with the epoxy groups of the sizing [14].

#### 3.2 Relaxation-induced piezoresistive behavior of monofilament composites

The relaxation-induced piezoresistive behavior of single fiber composites with vinyl ester matrix are presented in Fig. 4. For all composites, the initial stress was fixed at  $\sigma_0 = 15$  MPa (corresponding to a strain of 0.4 %, i.e.,  $\sim 40$  % of the ultimate strain). As seen in Fig. 4, all monofilament composites examined show a time-dependent electrical behavior in response to the stress relaxation. During the relaxation process CF/VER (Fig. 4a) exhibit a decrease of  $\sim 16$  % of the initial applied stress ( $\Delta\sigma/\sigma_0$ ) under constant strain, accompanied with an increase of  $\sim 1.4$  % in the fractional electrical resistance ( $\Delta R/R_0^r$ ) for  $t = 120$  min.

On the other hand, CNTF/VER composites (Fig. 4b) exhibit a decrease of  $\sim 22$  % of the initial applied stress, accompanied with a decrease of  $\sim 0.5$  % in the fractional electrical resistance for  $t = 40$  min; after those initial 40 min of stress relaxation, the electrical resistance of the composite exhibits certain oscillations that snap  $\Delta R/R_0^r$  back to  $\sim 0.3$  % for  $t = 120$  min. These oscillations indicate the presence of (sudden) irreversible phenomena in the fiber and fiber/matrix interphase, such as breakage or rearrangements of some contact points between the network of individual MWCNTs which

constitute the FCNT. These kind of irreversible phenomena occur because the strain in the material has been held constant for prolonged time periods (< 40 min).

For GF-CNT/VER monofilament composites (Fig. 4c), the relaxation behavior exhibit a decrease of ~18 % of the initial applied stress, accompanied with a decrease of ~16 % in electrical resistance for  $t = 120$  min. These changes in electrical resistance are an order of magnitude higher than those observed for the other two fibers, indicating that GF-CNT renders more sensitivity to this material system than CF or CNTF. This higher electrical sensitivity for GF-CNT is most likely due to the discontinuous character of the conducting elements (MWCNTs) on the GF.

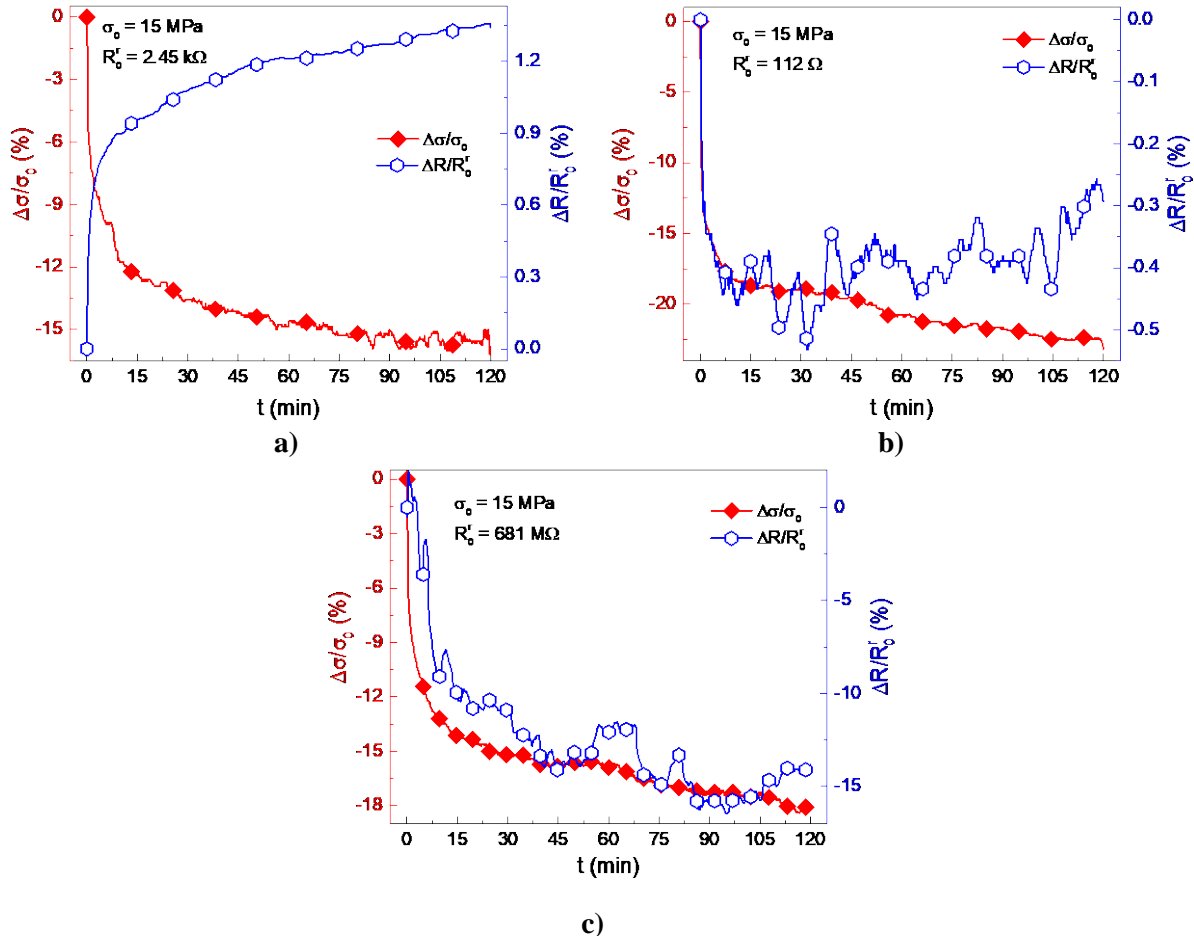


Figure 4: Relaxation-induced piezoresistive behavior of monofilament composites.  
a) CF/VER, b) CNTF/VER, c) GF-CNT/VER.

The different electrical behavior and sensitivity to stress relaxation observed for each of the different embedded fibers can be explained through the stress distribution around the fiber during the relaxation process, and the very different architectures at the nanoscale, as well as formed interphases [19]. When a uniaxial tensile stress/strain is applied to a monofilament composite, the large mismatch in elastic properties and the Poisson's contraction generate a radial compression stress in the fiber [20-23]. For the case of CF/VER, this radial compressive stresses and contraction of the cross-sectional area of the fiber by the Poisson's effect yields an increase in the electrical resistance of the monofilament composite, which evolves with time (Fig. 4a). The situation is quite different for CNTF (Fig. 4b), given its porous architecture. MWCNT yarns comprise millions of (discontinuous) bundled nanotubes twisted in a fiber architecture with about 5-40 CNT-to-CNT contact points per  $\mu\text{m}$  (depending on its density) and a large amount of voids, which defines its porosity [16]. The yarn porosity considers the volume fraction of spaces between the CNTs, and it has been shown that the fiber electrical conductivity is a strong function of the yarn porosity [16]. A radial compressive stress

applied to such a fiber architecture for prolonged times yields a decrease in the fiber porosity due to radial compressive stresses and contraction of the its cross-sectional area by the Poisson's effect, with the concomitant increase in the fiber conductivity. It is important to note that if the axial deformation applied is maintained for the longer times (greater than 40 min, as seen in Fig. 4b), the radial compression stress can modify the fiber nanostructure and/or interphase and cause interfacial damage in the composite, causing irreversible modifications of the MWCNT bundled network comprising the yarn, with the consequent oscillations and increase in electrical resistance observed in Fig. 4b, see also [4,24]. For the case of the GF-CNT the conducting network formed by the MWCNTs forms a discontinuous layer (both radially and longitudinally) on the GF fiber surface, see Fig. 3c. The separation between MWCNTs and between these layers affects the effective electrical resistance of the fibers, and if the separation between CNTs increase the electrical resistance increases too. During the relaxation process, the Poisson's effect and the radial compression stress on the fiber causes a rearrangement of the MWCNT network increasing the packing of the CNT layers (densifying them), with the consequent decrease of  $R$ . This trend continues for prolonged times up to 120 min, with small oscillations in  $R$  for long times that could indicate rupture of conductive paths and the beginning of interfacial failure (Fig. 4c) [4,24,25].

#### 4 CONCLUSIONS

The time-dependent electrical behavior of monofilament vinyl ester (VER) composites comprising carbon fibers (CF), carbon nanotube fibers (CNTF) and MWCNT-modified glass fibers (GF-CNT) subjected to stress relaxation at a constant strain of 0.4% has been investigated. Under time-dependent relaxation experiments, CF/VER monofilament composites exhibited a decrease of ~16 % of the initial applied stress (15 MPa), accompanied with an increase of electrical resistance of ~1.4 %. CNTF/VER composites exhibit a decrease of ~22 % of the initial applied stress, accompanied with a decrease of electrical resistance of ~0.5 %. GF-CNT/VER composites exhibit a decrease of ~20 % of the initial applied stress, accompanied with a decrease of electrical resistance of ~16 %. This indicates that the glass fiber modified by discontinuous MWCNTs is more sensitive to stress relaxation experienced by the polymer matrix. It was also found that exposing the CNTF/VER and CR/VER composite material to prolonged relaxation times ( $> 40$  min) at this strain level (0.4%) yield irreversible phenomena in these monofilament composites, which display as oscillations in the electrical resistance of the composites. The significantly different time-dependent piezoresistive trends observed under stress relaxation are ascribed to the significantly different fiber architecture at the nanoscale.

#### ACKNOWLEDGEMENTS

This work was supported by CONACYT grants No. 220513 and No. 188089 (CIAM) granted to Dr. Avilés.

#### REFERENCES

- [1] Paipetis A., Kostopoulos V., *Carbon Nanotube Enhanced Aerospace Composite Materials*, Springer, New York, USA, 2013.
- [2] Bakis C. E., Bank L. C., Brown V. L., Cosenza E., Davalos J. F., Lesko J. J., et al., Fiber-Reinforced Polymer Composites for Construction - State of the Art Review, *Journal of Composites for Construction*, **6**, 2002, pp.73-87 (doi: [10.1061/\(asce\)1090-0268\(2002\)6:2\(73\)](https://doi.org/10.1061/(asce)1090-0268(2002)6:2(73)))
- [3] Thostenson E. T., Ziaee S., Chou T.-W., Processing and electrical properties of carbon nanotube/vinyl ester nanocomposites, *Composites Science and Technology*, **69**, 2009, pp.801-804 (doi: [10.1016/j.compscitech.2008.06.023](https://doi.org/10.1016/j.compscitech.2008.06.023))
- [4] Wang X., Fu X., Chung D. D. L., Strain sensing using carbon fiber, *Journal of Materials Research*, **14**, 1999, pp.790-802 (doi: [10.1557/jmr.1999.0105](https://doi.org/10.1557/jmr.1999.0105))
- [5] Wen J., Xia Z., Choy F., Damage detection of carbon fiber reinforced polymer composites via electrical resistance measurement, *Composites Part B: Engineering*, **42**, 2011, pp.77-86 (doi: [10.1016/j.compositesb.2010.08.005](https://doi.org/10.1016/j.compositesb.2010.08.005))

- [6] Abot J. L., Alos T., Belay K., Strain dependence of electrical resistance in carbon nanotube yarns, *Carbon*, **70**, 2014, pp.95-102 (doi: [10.1016/j.carbon.2013.12.077](https://doi.org/10.1016/j.carbon.2013.12.077))
- [7] Georgousis G., Pandis C., Kalamiotis A., Georgopoulos P., Kyritsis A., Kontou E., et al., Strain sensing in polymer/carbon nanotube composites by electrical resistance measurement, *Composites Part B: Engineering*, **68**, 2015, pp.162-169 (doi: [10.1016/j.compositesb.2014.08.027](https://doi.org/10.1016/j.compositesb.2014.08.027))
- [8] Zhang C., Zhu J., Ouyang M., Ma C., Sumita M., Conductive network formation and electrical properties of poly(vinylidene fluoride)/multiwalled carbon nanotube composites: Percolation and dynamic percolation, *Journal of Applied Polymer Science*, **114**, 2009, pp.1405-1411 (doi: [10.1002/app.30729](https://doi.org/10.1002/app.30729))
- [9] Liu L., Ma P.-C., Xu M., Khan S. U., Kim J.-K., Strain-sensitive Raman spectroscopy and electrical resistance of carbon nanotube-coated glass fibre sensors, *Composites Science and Technology*, **72**, 2012, pp.1548-1555 (doi: [10.1016/j.compscitech.2012.06.002](https://doi.org/10.1016/j.compscitech.2012.06.002))
- [10] Boehle M., Jiang Q., Li L., Lagounov A., Lafdi K., Carbon nanotubes grown on glass fiber as a strain sensor for real time structural health monitoring, *International Journal of Smart and Nano Materials*, **3**, 2012, pp.162-168 (doi: [10.1080/19475411.2011.651509](https://doi.org/10.1080/19475411.2011.651509))
- [11] Sebastian J., Schehl N., Bouchard M., Boehle M., Li L., Lagounov A., et al., Health monitoring of structural composites with embedded carbon nanotube coated glass fiber sensors, *Carbon*, **66**, 2014, pp.191-200 (doi: [10.1016/j.carbon.2013.08.058](https://doi.org/10.1016/j.carbon.2013.08.058))
- [12] Cheap tubes Inc., Multi Walled Nanotubes-MWNTs 30-50nm Specifications. Grafton, USA, 2014. <http://www.cheaptubes.com/>. Fecha de consulta: Mayo del 2014.
- [13] Avilés F., Cauich-Rodríguez J. V., Moo-Tah L., May-Pat A., Vargas-Coronado R., Evaluation of mild acid oxidation treatments for MWCNT functionalization, *Carbon*, **47**, 2009, pp.2970-2975 (doi: [10.1016/j.carbon.2009.06.044](https://doi.org/10.1016/j.carbon.2009.06.044))
- [14] Ku-Herrera J. J., Avilés F., Nistal A., Cauich-Rodríguez J. V., Rubio F., Rubio J., et al., Interactions between the glass fiber coating and oxidized carbon nanotubes, *Applied Surface Science*, **330**, 2015, pp.383-392 (doi: [10.1016/j.apsusc.2015.01.025](https://doi.org/10.1016/j.apsusc.2015.01.025))
- [15] Jayasinghe C., Amstutz T., Schulz M. J., Shanov V., Improved Processing of Carbon Nanotube Yarn, *Journal of Nanomaterials*, **2013**, 2013, pp.1-7 (doi: [10.1155/2013/309617](https://doi.org/10.1155/2013/309617))
- [16] Miao M., Electrical conductivity of pure carbon nanotube yarns, *Carbon*, **49**, 2011, pp.3755-3761 (doi: [10.1016/j.carbon.2011.05.008](https://doi.org/10.1016/j.carbon.2011.05.008))
- [17] Chung D., *Carbon Fiber Composites*, Butterworth-Heinemann, Boston, USA, 1994.
- [18] Ku-Herrera J. J., May-Pat A., Avilés F., An Assessment of the Role of Fiber Coating and Suspending Fluid on the Deposition of Carbon Nanotubes onto Glass Fibers for Multiscale Composites., *Advanced Engineering Materials*, **18**, 2016, pp.963-971 (doi: [10.1002/adem.201500389](https://doi.org/10.1002/adem.201500389))
- [19] Sui X., Greenfeld I., Cohen H., Zhang X., Li Q., Wagner H. D., Multilevel composite using carbon nanotube fibers (CNTF), *Composites Science and Technology*, **137**, 2016, pp.35-43 (doi: [10.1016/j.compscitech.2016.10.011](https://doi.org/10.1016/j.compscitech.2016.10.011))
- [20] Ho H., Drzal L. T., Non-linear numerical study of the single-fiber fragmentation test. Part I: Test mechanics, *Composites Engineering*, **5**, 1995, pp.1231-1244 (doi: [10.1016/0961-9526\(95\)00065-u](https://doi.org/10.1016/0961-9526(95)00065-u))
- [21] Nairn J. A., Liu Y. C., Stress transfer into a fragmented, anisotropic fiber through an imperfect interface, *International Journal of Solids and Structures*, **34**, 1997, pp.1255-1281 (doi: [10.1016/s0020-7683\(96\)00065-0](https://doi.org/10.1016/s0020-7683(96)00065-0))
- [22] Nairn J. A., A variational mechanics analysis of the stresses around breaks in embedded fibers, *Mechanics of Materials*, **13**, 1992, pp.131-154 (doi: [10.1016/0167-6636\(92\)90042-c](https://doi.org/10.1016/0167-6636(92)90042-c))
- [23] Xiaojun W., Chung D. D. L., Residual stress in carbon fiber embedded in epoxy, studied by simultaneous measurement of applied stress and electrical resistance, *Composite Interfaces*, **5**, 1997, pp.277-281 (doi: [10.1163/156855498x00199](https://doi.org/10.1163/156855498x00199))
- [24] Lee S. I., Yoon D. J., Lee S. S., Park J. M., Cure Monitoring and Stress-Strain Sensing of Single-Carbon Fiber Composites by the Measurement of Electrical Resistance, *Key Engineering Materials*, **297-300**, 2005, pp.676-684 (doi: [10.4028/www.scientific.net/KEM.297-300.676](https://doi.org/10.4028/www.scientific.net/KEM.297-300.676))
- [25] Zhang J., Zhuang R., Liu J., Mäder E., Heinrich G., Gao S., Functional interphases with multi-walled carbon nanotubes in glass fibre/epoxy composites, *Carbon*, **48**, 2010, pp.2273-2281 (doi: [10.1016/j.carbon.2010.03.001](https://doi.org/10.1016/j.carbon.2010.03.001))